CHEMISTRY OF MATERIALS
Communication

Chem. Mater. **2010,** *22,* 4835–4837 4835
DOI:10.1021/cm101342r

Chemical Aerosol Flow Synthesis of Hollow Metallic Aluminum Particles

Richard J. Helmich and Kenneth S. Suslick*

Department of Chemistry, University of Illinois at Urbana−Champaign, 600 South Mathews Avenue, Urbana, Illinois 61802

Received May 12, 2010
Revised Manuscript Received August 3, 2010

The synthesis and use of finely divided aluminum powder has long been and continues to be of importance for energetic materials[1] because of the high heat of reaction[2] to form aluminum oxide, 31 kJ g^{-1}. There has been an upsurge of interest in submicrometer morphologies of Al for use in high energy nanocomposites (i.e., nanothermite[3] and other highly energetic mixtures[4,5] for explosives or propellants) and for use in hydrogen storage.[6]

Aerosol syntheses have been demonstrated to be a versatile and inexpensive tool used to create various types of nanomaterials including nitrides, oxides, chalcogenides, and carbon materials with many different morphologies and uses.[7,8] Aerosol syntheses of submicrometer metallic particles, however, are not common, and the synthesis of small aluminum particles have generally been in solution[9] or using expensive and energy intensive aerosol techniques (e.g., laser ablation, electrical exploding wires, etc.).[10]

In this communication, we report the synthesis of hollow metallic aluminum particles using a modified chemical aerosol flow synthesis (CAFS) technique[11] without the use of templating agents. A solution containing trimethylamine aluminum hydride (TMAH) in toluene was sonicated at 1.65 MHz to produce a fine mist of micrometer-sized droplets. The mist was carried by flowing argon into a heated glass tube where it combined with $TiCl_4$ vapor; $TiCl_4$ has been shown previously to catalyze the decomposition of alane (AlH_3) into metallic aluminum particles.[9] The resulting product was collected in bubblers filled with toluene, which are relatively inefficient: the collection efficiency of the system was ∼30% based on aluminum with typical yields of 200−500 mg of Al particles from 25 mL of precursor solution; the use of an electrostatic precipitator would significantly improve the collection efficiency. A schematic diagram of the CAFS system and detailed synthesis information is given in the Supporting Information (Figure S2).

The SEM and TEM images in Figure 1 shows the hollow morphology of the CAFS reaction products from the mist generated from 1 M TMAH when the aerosol was heated. Over the range of 100 to 200 °C, the morphology of the particles (i.e., wall thickness and particle size) did not change dramatically: sphere size is ∼300 nm and shell thickness ∼25 nm. Particles synthesized at lower temperatures, however, had a larger number of pores into the interior of the particles and showed more broken particles.

The effect of precursor solution concentration was investigated by nebulizing TMAH solutions varying between 0.5 and 2 M. Similar to the effects of increasing the synthesis temperature, TEM images showed that the particles become less porous with increasing precursor concentration (see Figure S3 in the Supporting Information) and that small amounts of Ti and Cl get trapped in the interior of nonporous particles created as observed by STEM EDX line scan analysis (Figure 2).

Further TEM and XPS analysis revealed the surface of the particles were passivated with a ∼5 nm thick layer of oxidized aluminum (Figures 3 and 4). Surface analysis with XPS showed aluminum peaks characteristic of both oxidized and metallic aluminum. A peak at 199 eV was attributed to residual surface chlorine originating from

*Corresponding author.

(1) (a) Russell, M. S. *The Chemistry of Fireworks*; Royal Society of Chemistry: Cambridge, U.K., 2002.(b) Fischer, S. H.; Grubelich, M. C. *Proceedings of the 24th International Pyrotechnics Seminar*; Monterey, CA; International Pyrotechnics Society, 1998.(c) Cooper, P. *Explosives Engineering*; Wiley-VCH: New York, 1996.
(2) Atkins, P.; Paula, J. D. *Physical Chemistry*, 7th ed.; W. H. Freeman and Company: New York, 2002.
(3) (a) Dreizin, E. L. *Prog. Energy Combust. Sci.* **2009**, *35*, 141–167. (b) Apperson, S. J.; Bezmelnitsyn, A. V.; Andrey, V.; Thiruvengadathan, R.; Gangopadhyay, K; Gangopadhyay, S; Balas, W. A.; Anderson, P. E.; Nicolich, S. M. *J. Prop. Power* **2009**, *25*, 1086–1091. (c) Puszynski, J. A. *J. Therm. Anal. Calorim.* **2009**, *96*, 677–685.
(4) (a) Foley, T. J.; Johnson, C. E.; Higa, K. T. *Chem. Mater.* **2005**, *17*, 4086–4091. (b) Guo, L.; Song, W.; Hu, M.; Xie, C.; Chen, X. *Appl. Surf. Sci.* **2008**, *254*, 2413–2417. (c) Jouet, R. J.; Warren, A. D.; Rosenberg, D. M.; Bellitto, V. J.; Park, K.; Zachariah, M. R. *Chem. Mater.* **2005**, *17*, 2987–2996. (d) Malchi, J. Y.; Foley, T. J.; Yetter, R. A. *Appl. Mater. Interf.* **2009**, *1*, 2420–2423. (e) Prakash, A.; McCormick, A. V.; Zachariah, M. R. *Adv. Mater.* **2005**, *17*, 900–903. (f) Zamkov, M. A.; Conner, R. W.; Dlott, D. D. *J. Phys. Chem. C* **2007**, *111*, 10278–10284.
(5) (b) Steinhauser, G.; Klapötke, T. M. *Angew. Chem., Int. Ed.* **2008**, *47*, 3330–3347.
(6) Ritter, J. A.; Ebner, A. D.; Wang, J.; Zidan, R. *Mater. Today* **2003**, *6*, 18–23.
(7) (a) Kodas, T. T.; Hampden-Smith, M. *Aerosol Processing of Materials*; Wiley-VCH: New York, 1999. (b) Bang, J. H.; Suslick, K. S. *Adv. Mater.* **2010**, *22*(10), 1039–1059.
(8) (a) Bang, J. H.; Helmich, R. J.; Suslick, K. S. *Adv. Mater.* **2008**, *20*, 2599–2603. (b) Strobel, R; Baiker, A.; Pratsinis, S. E. *Adv. Powder Technol.* **2006**, *17*, 457–480. (c) Skrabalak, S. E.; Suslick, K. S. *J. Am. Chem. Soc.* **2006**, *128*, 12642–12643. (d) Skrabalak, S. E.; Suslick, K. S. *J. Am. Chem. Soc.* **2005**, *127*, 9990–9991. (e) Okuyama, K.; Lenggoro, I. W. *Chem. Eng. Sci.* **2003**, *58*, 537–547. (f) Tsai, S. C.; Long, Y. L.; Tsai, C. S.; Yang, C. C.; Chiu, W. Y.; Lin, H. M. *J. Mater. Sci.* **2004**, *39*, 3647–3657.
(9) Higa, K. T.; Johnson, C. E.; Hollins, R. A. U S. Patent 5 885 321 1996.
(10) (a) Ivanov, Y. F.; Osmonoliev, M. N.; Sedoi, V. S.; Arkhipov, V. A.; Bondarchuk, S. S.; Vorozhtsov, A. B.; Korotkikh, A. G.; Kuznetsov, V. T. *Propellants, Explos., Pyrotech.* **2003**, *28*, 319–333. (b) Jayaraman, K.; Anand, K. V.; Bhatt, D. S.; Chakravarthy, S. R.; Sarathi, R. *J. Propul. Power* **2009**, *25*, 471–481. (c) Park, K.; Rai, A.; Zachariah, M. R. *J. Nanopart. Res.* **2006**, *8*, 455–464.
(11) (a) Didenko, Y. T.; Suslick, K. S. *J. Am. Chem. Soc.* **2005**, *127*, 12196–12197.(b) Didenko, Y. T.; Suslick, K. S. U.S. Patent 7 160 489, Jan. 9, 2007. (c) Bang, J. H.; Suh, W. H.; Suslick, K. S. *Chem. Mater.* **2008**, *20*, 4033–4038.

Published on Web 08/18/2010

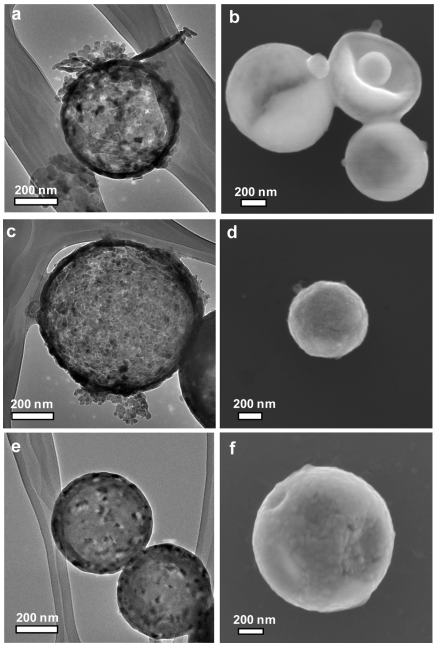

Figure 1. TEM and SEM images of hollow metallic aluminum particles prepared by chemical aerosol flow synthesis from 1 M trimethylamine aluminum hydride at various temperatures: (a, b) 100, (c, d) 150, and (e, f) 200 °C.

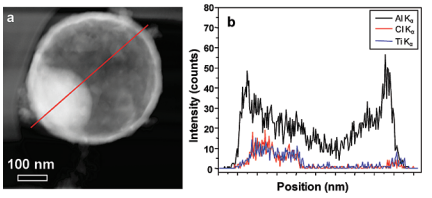

Figure 2. (a) HAADF-STEM image and (b) EDX line scan analysis of a particle prepared from 1.5 M TMAH at 150 °C. The red line in image (a) indicates the line scan analysis path.

the $TiCl_4$ catalyst. While peaks at the binding energy for titanium were barely discernible for porous shells, hollow Al spheres without porosity (i.e., Figure 1e, f) showed Ti 2p peaks that match with previously reported binding energies for $TiCl_4$ (see Figure S4 in the Supporting Information). Surface area and N_2 adsorption analysis was performed on several samples. The surface area calculate for samples were relatively low, typically >20 m^2/g. Full isotherms were measured on samples both with porous and with nonporous morphologies as determined by TEM; all samples showed Type II (i.e., nonmicroporous) adsorption isotherms, as expected.[12]

Attempts to create particles with alternative passivating agents, such as long chain carboxylic acids, did not prevent the formation of a surface oxide layer. In spite of stringent attempts to eliminate all sources of oxygen from the product during workup, only particles with ~5 nm thick layer of aluminum oxide were formed even in the presence of other passivating agents. The crystallinity of the products was examined using X-ray powder diffraction analysis, and the Debye-Sherrer formula was used to calculate the domain size of the crystallites. All reaction products showed diffraction peaks matching fcc metallic aluminum. No additional

(12) Sing, K. S. W.; Everett, D. H.; Haul, R. A.; Moscou, L.; Pierotti, R. A.; Rouquerol, J.; Siemieniewska, T. *Pure Appl. Chem.* **1985**, *57*, 603–619.

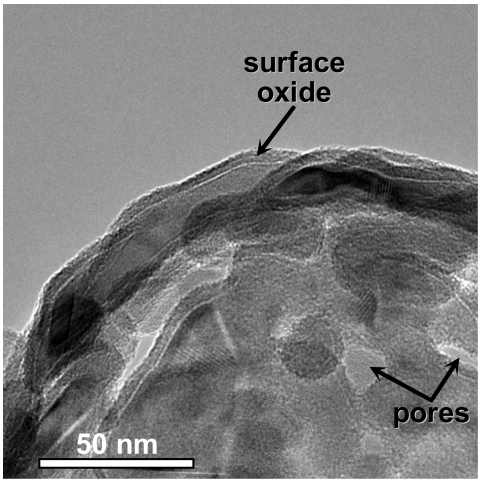

Figure 3. TEM image showing surface layer of oxidized alumium and pores leading to the interior of the particle from a sample synthesized from 1 M TMAH at 100 °C.

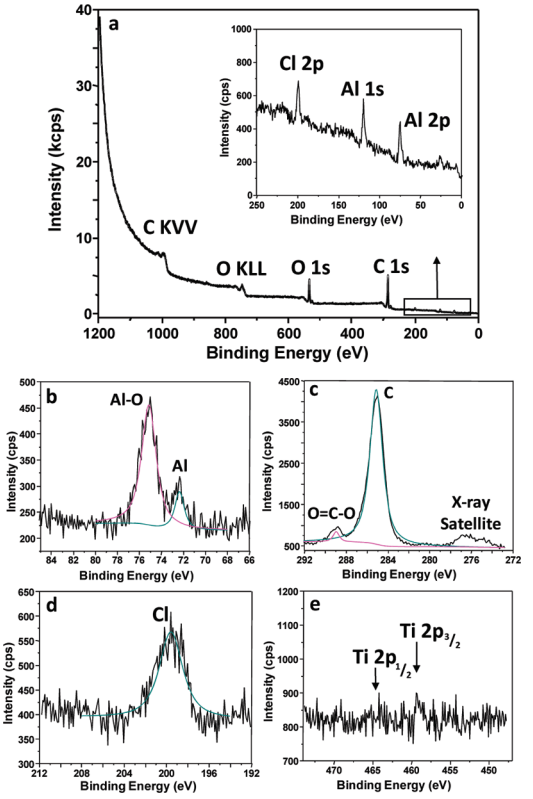

Figure 4. XPS spectra of hollow aluminum particles prepared from 1.0 M TMAH at 100 °C. (a) Survey spectrum, (b−e) high-resolution spectra of elements Al, C, Cl, and Ti, respectively.

peaks corresponding to aluminum oxide phases were seen in the XRD pattern, consistent with a thin amorphous surface oxide layer (Figure 5). Analysis of crystallite size as a function of synthesis temperature and precursor concentration showed that smaller crystalline domains were formed at higher temperature. Increasing the concentration of the TMAH precursor solution under isothermal conditions increased the crystallite domain sizes (see Figure S6 in the Supporting Information).

On the basis of the morphology and the CAFS synthesis method, we proposed a simple model for the formation of these hollow aluminum particles (see Figure S7

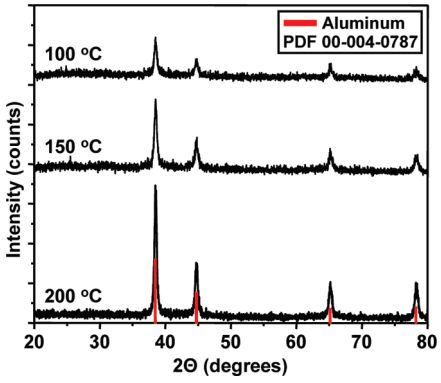

Figure 5. Powder X-ray diffraction patterns for products from 1 M TMAH created at 100−200 °C. Diffraction lines were matched to metallic aluminum (ICDD PDF card 00−004−0787).

Scheme 1. Chemical Reaction for the Catalyzed Decomposition of Trimethylamine Aluminum Hydride (TMAH) by Titanium Tetrachloride

$$(CH_3)_3N{:}AlH_3 \xrightarrow{TiCl_4} Al + N(CH_3)_3 + 3/2\ H_2$$

in the Supporting Information). The formation of aluminum begins as $TiCl_4$ vapor diffuses into the surface of TMAH droplets, which initiates formation of aluminum nanoparticles on the surface of the droplets (Scheme 1). We hypothesize that the evolution of gas (i.e., H_2 and $N(CH_3)_3$) during the decomposition of the TMAH precursor forms very small bubbles that carry adhered solid particles to the surface of the droplet. This is consistent with the eventual formation of the solid shell around a hollow interior that is observed.

At low temperatures or high precursor concentrations, the hollow particles consist of agglomerates of larger aluminum nanoparticles with macropores to the interior. At higher temperatures or lower precursor concentrations, the Al shell is smoother and appears to be nonporous. The nonporous shells trap some of the residual solvent and $TiCl_4$ within the particles (see Figure S7 in the Supporting Information).

Thermal analyses of the hollow Al particles were performed in both nitrogen and oxygen atmospheres (Figure 6). Samples heated to ~550 °C under N_2 showed a loss of ~30 wt % without any significant exothermic reactions. In comparison, the same sample run under O_2 (23% O_2 in N_2) showed a broad exothermic reaction suggesting the desorption and combustion of solvent trapped in the interior of particles with nonporous surfaces within the sample; similar behavior is observed for oleic-acid-coated solid Al nanoparticles.[13] At temperatures above 550 °C, the sample under N_2 shows only a very weak exothermic peak and small mass increase, whereas heating under O_2 showed two strongly exothermic reaction peaks and a corresponding mass increase due to rapid formation of Al_2O_3. The two-step oxidation behavior has been reported previously[14] and is attributed to initial formation and thickening of an amophous oxide layer with crystallization into γ-Al_2O_3 followed by subsequent formation of γ-Al_2O_3 platelets and exposure of additional aluminum metal.[14]

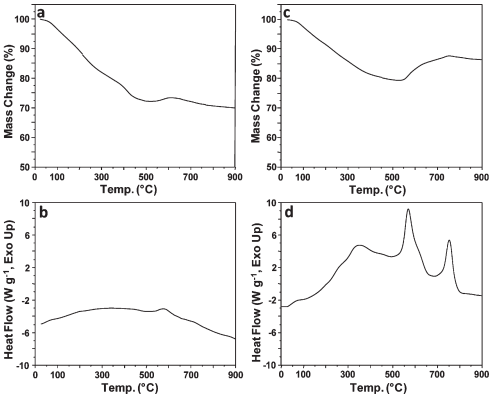

Figure 6. Differential scanning calorimetry (DSC) and thermogravimetric analysis (TGA) of aluminum spheres from 1.5 M trimethylamine aluminum hydride at 150 °C (an b) under N_2 atmosphere; (c, d) under 23% O_2 in N_2; linear heating rates at 20 K/min.

In the absence of heating, the hollow aluminum spheres are stable: under ambient conditions (~25 °C, ~30% RH), no measurable changes in oxide thickness occur even after five months (see Figure S8 in the Supporting Information). In addition, the active aluminum content was measured using a previously reported redox titration method.[15] After storage at room temperature under air for 5 months, two samples were analyzed, and found to contain 72 and 85 wt % active aluminum for materials prepared at 100 and 200 °C, respectively.

In conclusion, we have discovered a novel synthesis of hollow, metallic aluminum particles using a modified chemical aerosol flow synthesis technique. The porosity of the shells could be controlled by adjusting the TMAH precursor solution concentration or the synthesis temperature. Attempts to create particles passivated with capping agents such as long alkyl chain carboxylic acids were unsuccessful, and only particles with a ~5 nm thick layer of aluminum oxide were formed. The CAFS technique has advantages when compared to previously methods for synthesizing nanoparticles of metallic aluminum. CAFS is simple, energy efficient, and highly scalable in comparison to previously reported syntheses, i.e., exploding wire and evaporation methods, which are energy intensive, require complex vacuum apparatuses, and are difficult to scale-up. Future work is underway to use this technique to create composite materials that contain oxidizers such as Teflon particles or metal oxides.

Acknowledgment. These studies were supported by the NSF, DMR 09-06904. Characterizations were carried out in the Center for Microanalysis of Materials at the University of Illinois at Urbana−Champaign, which is partially supported by the U.S. DOE under Grants DE-FG02-07ER46453 and DE-FG02-07ER46471.

Supporting Information Available: Detailed synthesis information, a schematic of the CAFS setup, and additional materials characterizations (PDF). This material is available free of charge via the Internet at http://pubs.acs.org.

(13) Fernando, K. A. S.; Smith, M. J.; Harruff, B. A.; Lewis, W. K.; Guliants, E. A.; Bunker, C. E. *J. Phys. Chem. C* **2008**, *113*, 500–503.
(14) Trunov, M. A.; Schoenitz, M.; Dreizen, E. L. *Combust. Theory Modell.* **2006**, *10*, 603–623.
(15) Chen, L.; Song, W.; Lv, J.; Chen, X.; Xie, C. Mater. Chem. Phys., *120*, 670−675.